ISBN: 978-3-95450-208-0 doi:10.18429/JACoW-IPAC2019-TUPTS080

# BEAM DYNAMICS STUDIES OF AN APEX2-BASED PHOTOINJECTOR

C. E. Mitchell*, H. Feng, D. Filippetto, M. J. Johnson, A. R. Lambert, D. Li, T. Luo,
F. Sannibale, J. W. Staples, S. Virostek, R. Wells
Lawrence Berkeley National Laboratory, Berkeley, CA 94720, USA

*Abstract*

APEX2 is a proposed normal conducting radio-frequency (RF) electron gun operating in the very high frequency (VHF) range in continuous wave (CW) mode, designed to drive applications that require both high beam brightness and high repetition rate, such as free electron lasers (such as LCLS-II-HE), ultra-fast electron diffraction, and microscopy. The gun consists of a two-cell RF cavity operating at 162.5 MHz with a cathode field of 34 MV/m, together with an embedded focusing solenoid. We study the beam dynamics in an APEX2-based photoinjector (up to 20 MeV), targeting a transverse 95% beam emittance of 0.1 μm at 12.5 A peak current for the case of 100 pC charge for FEL applications. The high cathode field leads to enhanced beam brightness, while the increased gun exit energy of 1.5 MeV reduces the effects of space charge, and possibly eliminates the need for an RF buncher. The embedded solenoid is designed to control the transverse beam size while minimizing emittance growth due to geometric aberrations. As a result, the transverse beam performance targets are achieved, and ongoing work will further optimize longitudinal beam quality for downstream FEL transport.

## APEX2 GUN AND PHOTOINJECTOR

Figure 1 illustrates the current APEX2 gun design, consisting of two 162.5 MHz RF cells with embedded bucking and focusing solenoids. The cells are optimized to achieve a peak cathode accelerating field of 34 MV/m, while maintaining acceptable wall power density and providing a beam kinetic energy of 1.5-2.0 MeV. Details of the RF and mechanical gun design are described elsewhere [1, 2]. Figure 2 illustrates the resulting fields along the axis in the gun region. The focusing field of the embedded solenoid penetrates into the gap of the second cell, while a bucking solenoid is used to zero this field at the cathode.

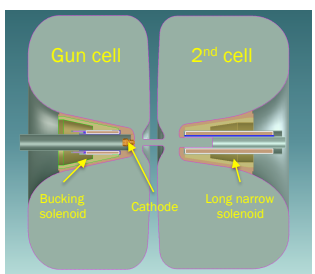


Figure 1: Schematic of the APEX2 162.5 MHz CW RF gun structure with embedded solenoids.

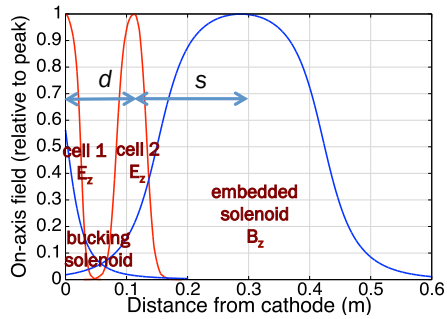


Figure 2: On-axis field profiles from the cathode through the gun exit. (Red) Accelerating fields. (Blue) Focusing fields.

The primary purpose of these studies was to to aid in selection of the APEX2 gun configuration (comparing single-cell, double-cell shared wall, and split double-cell options) and element spacings (parameters $d$ and $s$ in Fig. 2) based on achieving optimal beam quality in a simple photoinjector. Figure 3 illustrates the layout used, which is a modification of the experimental APEX injector layout [3]. Three 7-cell normal-conducting 1.3 GHz cavities are used to accelerate the beam to an energy of 15-20 MeV. Previous studies indicated that similar emittance and peak current could be obtained with or without the use of an RF buncher [4], so for these studies, the APEX RF buncher section has been removed.

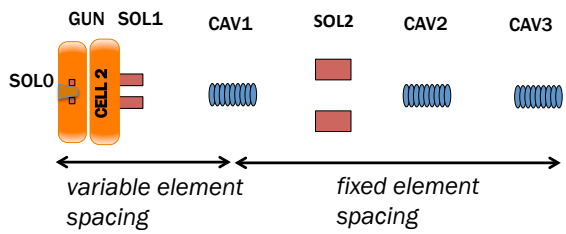


Figure 3: Photoinjector layout used for studies of beam dynamics up to an energy of ~20 MeV.

Table 1 lists beam performance targets motivated by free electron laser (FEL) applications (such as LCLS-II-HE). Here, our focus is primarily on the transverse emittance. As a measure of longitudinal beam quality, we use the higher-order momentum spread, defined as $\sigma_{\hat{p}}$, where $\hat{p} = p_z - p_z(z)$, with $p_z(z)$ a quadratic fit to the longitudinal phase space (the longitudinal rms momentum spread after removing linear and quadratic correlations) [5].

## BEAM PERFORMANCE OPTIMIZATION

A multi-objective genetic algorithm coupled with Astra [6, 7] was used to tune injector settings to find a nominal

* ChadMitchell@lbl.gov

ISBN: 978-3-95450-208-0 doi:10.18429/JACoW-IPAC2019-TUPTS080



Table 1: Beam Dynamics Targets

| Parameter | Value | |
|---|---|---|
| Bunch charge | 100 | pC |
| $\epsilon_{x,n}$ (95% projected) | ≤ 0.1 | µm |
| Peak current | ≥ 12 | A |
| Beam KE, gun exit | ≥ 1.5 | MeV |
| Beam KE, final | 15-20 | MeV |
| Higher-order $\sigma_p$ | < 10 | keV/c |

Table 2: Beam Performance (for the solution shown in Fig. 4)

| Parameter | Value | |
|---|---|---|
| $\epsilon_{x,n}$ (100% projected) | 0.1032 | µm |
| $\epsilon_{x,n}$ (95% projected) | 0.0874 | µm |
| Peak current | 12.5 | A |
| Beam KE, gun exit | 1.5 | MeV |
| Beam KE, final | 19.2 | MeV |
| Higher-order $\sigma_p$ | 6.70 | keV/c |

injector working point. The initial distribution is taken to be transversely Gaussian, truncated at a radius of $1\sigma_x$, with a thermal emittance of 0.6 µm/mm and longitudinally plateau with a rise time of 2 ps. The cathode field is always taken to be 34 MV/m (at RF crest).

The two objectives to be minimized are the transverse rms (100 %) projected emittance and the rms bunch length at the injector exit. A total of ~15 parameters are varied, including the RF phase of both gun cells (allowed to vary independently), the RF field amplitude in gun cell 2, the solenoid strengths, and the gradients and phases of the accelerating cavities. The initial beam size and pulse length are also allowed to vary. In addition, several spacings of the low-energy elements are considered (Fig. 3). During optimization, four constraints are imposed at the injector exit: $\epsilon_{x,n} \leq 0.8$ µm, $\sigma_z \leq 1.35$ mm, $\sigma_E \leq 200$ keV, and $\sigma_p \leq 10$ keV/c.

Figure 4 illustrates the best-performing solution so far obtained, while Table 2 lists the corresponding beam parameters. This suggests that such a gun design can, in principle, drive an injector that meets the targets in Table 1.

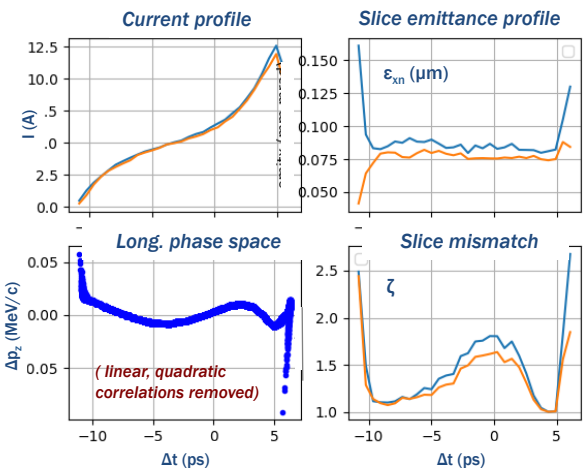


Figure 4: Best-performing 100 pC solution at the injector exit for the layout shown in Fig. 3.

## BEAM DYNAMICS STUDIES

This beam performance was achieved after considering several variations of gun and injector design. In particular, we investigated sensitivity of the final rms emittance to RF gun cell separation and to the position of the main focusing solenoid, parameters $d$ and $s$ in Fig. 2. In these studies, an APEX-style solenoid was used for the primary focusing (SOL1), and injector settings were re-optimized for several fixed values of $d$ and $s$. We found an optimal cell separation near $d = 11$ cm, with an emittance sensitivity of 5% over changes up to 6 cm (Fig. 5). In contrast, the emittance sensitivity to the main solenoid location $s$ is quite strong. Mechanical constraints (when using an APEX-style solenoid) required $s \geq 0.2$ m, resulting in a final projected emittance > 0.16 µm, more than 50% larger than the corresponding result with $s = 0.1$ m. This is due to emittance growth driven by geometric aberrations in the main focusing solenoid, as a result of the large beam size in SOL1, as seen in Fig. 6.

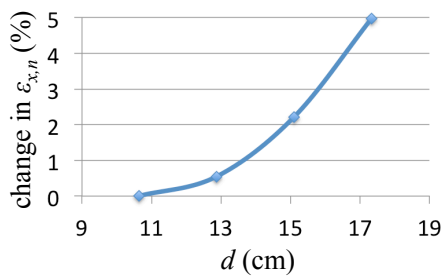


Figure 5: Sensitivity of the final beam emittance at injector exit to RF gun cell separation (relative to optimum).

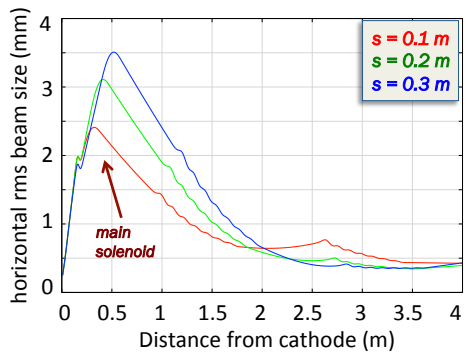


Figure 6: Horizontal rms beam size evolution, showing sensitivity to SOL1 location $s$. The beam size in SOL1 has strong consequences for third-order geometric aberrations.

ISBN: 978-3-95450-208-0 doi:10.18429/JACoW-IPAC2019-TUPTS080

To address this, three options were studied: 1) introduce an additional focusing solenoid at low energy between the two RF gun cells, to reduce the beam size and focusing field required in SOL1, 2) eliminate the second RF gun cell and place SOL1 adjacent to the gun cell exit, or 3) move SOL1 closer to the cathode by mechanically redesigning either the second gun cell or the solenoid. Options 1) and 2) each resulted in beams with (100% proj.) $\epsilon_{x,n} \approx 0.1$ µm at 12.5 A. In the case of Option 1), we found that a trade-off between aberrations in the two low-energy solenoids also greatly reduced the sensitivity to SOL1 location, allowing for greater design flexibility. However, for both Options 1)-2), the beam energy at the gun exit was significantly lower than our target (near 0.75 MeV). To explore Option 3), the nose cone of the second gun cell was thinned and a new, embedded solenoid design was developed, as shown in Fig. 1. This resulted in the performance shown in Table 2.

## SOLENOID ABERRATIONS

We characterize solenoid field quality using the following two integrals of the on-axis magnetic field:

$$I_1 = \int \left(\frac{B_z}{B_0}\right)^2 dz, \qquad I_2 = \int \left(\frac{1}{B_0}\frac{\partial B_z}{dz}\right)^2 dz, \quad (1)$$

where $B_0 = |B_z|_{\max}$. The solenoid focal length $f$ and quality factor $q_f$ are defined by:

$$k_{max} = \frac{B_0}{B\rho}, \qquad \frac{1}{f} = k_{max}^2 I_1, \qquad q_f = \frac{I_2}{2I_1}, \quad (2)$$

where $B\rho$ denotes the magnetic rigidity.

The emittance growth due to third-order geometric aberrations is then approximated for a given focal length $f$ by [8]:

$$\epsilon_{x,n}^{geom} \approx (\beta\gamma)\frac{q_f}{f}\kappa\sigma_x^4, \quad (3)$$

where $\kappa$, of order unity, is determined by the shape of the transverse beam profile.

The field $B_z/B_0$ of the narrow-bore embedded solenoid is shown in Fig. 7, together with corresponding result for the APEX solenoid design. For the embedded (APEX) solenoid, we find $I_1$ = 22.6 cm (15.8 cm) and $q_f$=27.0 m$^{-2}$ (72.6 m$^{-2}$), an improvement in $q_f$ by a factor of 2.7. The increased effective length, and the embedding of this solenoid into the nose code (Fig. 1) allows a penetrating focusing field that reduces the transverse expansion of the beam in the gun, reducing $\sigma_x$ at the location of SOL1 by ~ 10%. As a consequence of improved beam size control and solenoid field quality, the transverse emittance is improved by ~ 15%, nearly all of which appears in the slice emittance. In Fig. 7, results are shown for 10K particle simulations, and emittance values are 20% smaller at convergence (250K particles, as reported in Table 2).

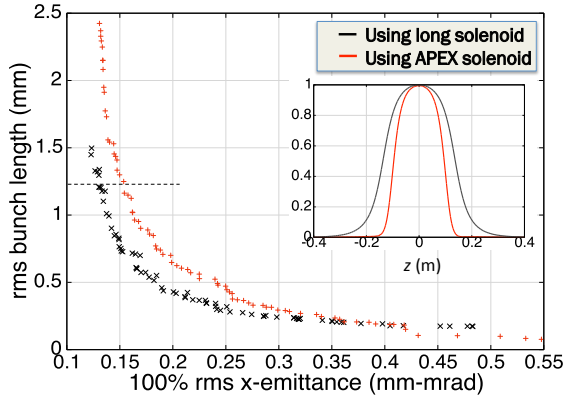


Figure 7: Pareto-optimal front illustrating beam performance using an APEX solenoid versus an embedded solenoid for SOL1. (Profiles of the on-axis magnetic field inset.)

## CONCLUSION

In comparison with APEX [3], the increased cathode field of APEX2 (34 MV/m) yields improved beam brightness at emission, while the increased gun energy (twice that of APEX) yields reduced sensitivity to nonlinear space charge fields. To preserve this brightness, the beam size must be tightly controlled, which is achieved using a new embedded solenoid design with improved transverse field quality, reducing third-order solenoid aberrations. The resulting simulated emittance at 20 MeV (0.1 µm) is half that of the optimized (simulated) APEX design for 100 pC bunches at 12 A. We plan to revisit the injector design, including the option of an RF buncher, and future work will focus on improving the beam longitudinal phase space and current profile. We also plan to consider optimization at higher and lower bunch charge, and injection into an RF cryomodule, bringing the beam energy up to ~100 MeV.

## ACKNOWLEDGEMENTS

This work was was supported by the U.S. Department of Energy Office of Science, Office of Basic Energy Sciences, under Contract No. DE-AC02-05CH11231, and made use of computer resources at the National Energy Research Scientific Computing Center.

## REFERENCES

[1] T. H. Luo *et al.*, "RF design of APEX2 cavities", presented at the IPAC'19, Melbourne, Australia, May 2019, paper TUPTS076, this conference.

[2] A. R. Lambert *et al.*, "Mechanical Design and Analysis of the Proposed APEX2 VHF CW Electron Gun", presented at the IPAC'19, Melbourne, Australia, May 2019, paper WEPRB084, this conference.

[3] F. Sannibale *al*, "High-Brightness Beam Tests of the Very High Frequency Gun at the Advanced Photo-injector EXperiment Test Facility at the Lawrence Berkeley National Laboratory ", *Rev. Sci. Instrum.*, vol. 90, p. 033304, 2019.

[4] F. Sannibale *et al.*, "Upgrade Possibilities for Continuous Wave RF Electron Guns Based on Room-Temperature Very High

ISBN: 978-3-95450-208-0 doi:10.18429/JACoW-IPAC2019-TUPTS080

Frequency Technology", *Phys. Rev. Accel. Beams*, vol. 20, p. 113402, 2017.

[5] C. E. Mitchell *et al.*, "RF Injector Beam Dynamics Optimization and Injected Beam Energy Constraints for LCLS-II", in *Proc. IPAC'16*, Busan, Korea, May 2016, pp. 1699–1702. doi:10.18429/JACoW-IPAC2016-TUPOR019

[6] K. Deb *et al.*, "A Fast and Elitist Multiobjective Genetic Algorithm: NSGA-II", *IEEE Trans. on Evol. Comp.*, vol. 60, p. 182, 2002.

[7] C. F. Papadopoulos *et al.*, "RF Injector Beam Dynamics Optimization for LCLS-II", in *Proc. IPAC'14*, Dresden, Germany, Jun. 2014, pp. 1974–1976. doi:10.18429/JACoW-IPAC2014-WEPRO015

[8] I. Bazarov *et al.*, "Comparison of DC and Superconducting RF Photoemission Guns for High Brightness High Average Current Beam Production", *Phys. Rev. Accel. Beams*, vol. 14, p. 072001, 2011.